A Molecular Quantum Description of Spin Alignments in Molecule-Based Ferrimagnets: Numerical Calculations of Thermodynamic Properties†

Daisuke Shiomi,§ Kazunobu Sato,‡ and Takeji Takui*,‡

Department of Materials Science and Department of Chemistry, Graduate School of Science, Osaka City University, Sumiyoshi-ku, Osaka 558-8585, Japan

Received: June 26, 2001; In Final Form: October 18, 2001

A physical picture of electron spin alignments in organic molecule-based ferrimagnets is given from numerical calculations of magnetic specific heat (C), magnetic entropy (S_{mag}), and magnetic susceptibility (χ) as functions of temperature (T) and static magnetic field (B) in terms of a Heisenberg Hamiltonian for an alternating spin chain. The numerical results are compared with those for atom-based ferrimagnets. One of the two kinds of spin sites in the chain represents an organic molecule with two $S = {}^1/_2$ spins, which are coupled to give a ground-state triplet ($S = 1$) biradical molecule. The biradical molecule is coupled with adjacent $S = {}^1/_2$ monoradicals by the intermolecular antiferromagnetic interactions. When the strength of the intermolecular antiferromagnetic interactions is dimerized along the chain, three peaks in the C vs T curve appear. Two of the three peaks shift to higher and lower temperatures with increasing magnetic field, B, indicating that one originates in the ferromagnetic nature and the other in the antiferromagnetic nature, respectively. The magnetic entropy, S_{mag}, exhibits 3-fold stepwise drops as T is lowered. One of the drops with the stationary value of $S_{mag} = k_B \ln 2$ corresponds to generation of an effective $S = {}^1/_2$ spin in the unit cell of the chain as a result of the coupling of adjacent $S = 1$ and $S = {}^1/_2$ spins. With the aid of quantum Monte Carlo simulations of magnetic susceptibility, χ, the ferrimagnetic spin alignment in the alternating molecular chains of biradicals and monoradicals is shown to be equivalent to the ferromagnetic alignment of the effective $S = {}^1/_2$ spins. A spin polarization effect affording the effective ferromagnetic interactions between the effective $S = {}^1/_2$ spins is demonstrated in terms of a simple Heisenberg model.

Introduction

Molecule-based magnets and other molecular functionality magnetics have received great interest in recent years.[1] More than thirty ferromagnets have been discovered in genuinely organic molecule-based materials[1] after the discovery of the first organic ferromagnet, *p*-NPNN.[2] Ferrimagnets have also been attracting attention as one of the facile approaches to organic magnets after the first proposal of Buchachenko in 1979.[3] The concept of organic ferrimagnetics is based on the tendency for organic open-shell molecules to have antiferromagnetic intermolecular interactions. The antiferromagnetic interactions would bring about antiparallel spin alignment between neighboring molecules with different magnetic moments to result in a possible ordered state with net magnetization. Magnetic phase transitions to a ferrimagnetic ordered state, however, have not been documented so far in organic molecular crystalline solids. This presents a remarkable contrast to the discovery of the organic molecular ferromagnets[1,2] with purely ferromagnetic intermolecular interactions and inorganic metal-based molecular ferrimagnets.[4] Meanwhile, a molecular complex of a ground-state triplet ($S = 1$) biradical and an $S = {}^1/_2$ monoradical has been synthesized,[5] with which Izuoka et al. have made a breakthrough in both organic molecule-based magnetics and materials science: An alternating chain structure of the two kinds of molecules with different spin quantum numbers has been achieved in the complex.[5] No phase transition to a bulk ferrimagnetic ordered state, however, has been observed.[5−7] Thus, molecule-based ferrimagnetics is still a long-standing issue in terms of materials challenge in chemistry. In the current study, a physical picture of the ferrimagnetic spin alignment in the molecule-based systems is proposed from numerical calculations of thermodynamic properties such as specific heat, entropy, and magnetic susceptibility.

Organic molecule-based magnetics is characterized by the following features:[6−10] In organic molecule-based magnetic materials, spin density is distributed over many atomic sites in an open-shell molecule, and hence, the intermolecular spin−spin interaction has a multicentered or multicontact nature. Furthermore, in most cases, intramolecular interactions in stable organic $S > {}^1/_2$ molecules are on the same order of magnitude as the intermolecular interactions in crystalline solid states. Such spin systems feature in the magnetic degree of freedom within the $S > {}^1/_2$ molecules and the spatial symmetry of intermolecular exchange interaction. The phenomenological spin Hamiltonian suitable for such organic molecule-based ferrimagnets in the presence of an applied static magnetic field, B, is given by

$$H_{mol} = \sum_{i=1}^{N}[-2J_1\mathbf{S}_{i,b1}\cdot\mathbf{S}_{i,b2} - 2J_2\mathbf{S}_{i,b2}\cdot\mathbf{S}_{i,m} - 2J'_2\mathbf{S}_{i,b1}\cdot\mathbf{S}_{i,m} - 2J_3\mathbf{S}_{i,m}\cdot\mathbf{S}_{i+1,b2} - 2J'_3\mathbf{S}_{i,m}\cdot\mathbf{S}_{i+1,b1} + g\mu_B B(S^z_{i,b1} + S^z_{i,b2} + S^z_{i,m})] \quad (1)$$

where $\mathbf{S}_{i,b1}$, $\mathbf{S}_{i,b2}$, and $\mathbf{S}_{i,m}$ denote the spin-${}^1/_2$ operators and N is

† Part of the special issue "Noboru Mataga Festschrift".

* To whom correspondence should be addressed. E-mail address: takui@sci.osaka-cu.ac.jp. Telephone number: +81-6-6605-2605. Fax number: +81-6-6605-3137.

§ Department of Materials Science.

‡ Department of Chemistry.

10.1021/jp0124387 CCC: $22.00
Published on Web 12/18/2001

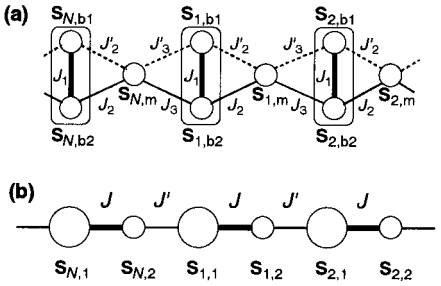

Figure 1. Heisenberg spin Hamiltonian of the ferrimagnetic chain with N repeating units. Panel a shows the multicentered ferrimagnetic chain, H_{mol} (eq 1), as a model for organic molecule-based ferrimagnets. The rounded rectangles are the biradical molecules with two unpaired electron spins ($S_{i,b1} = {}^1/_2$ and $S_{i,b2} = {}^1/_2$), which interact with the adjacent monoradicals with $S_{i,m} = {}^1/_2$. The thick solid line denotes the intramolecular interaction, J_1, while the thin solid and dashed lines denote the intermolecular interactions, J_2, J'_2, J_3, and J'_3. Panel b shows the atom-based ferromagnetic spin chain, H_{atom} (eq 2), composed of $S_{i,1} = 1$ and $S_{i,2} = {}^1/_2$ spins. J and J' denote the interatomic antiferromagnetic interactions. The periodic boundary condition is imposed for both panel a and panel b.

the number of unit cells. The Hamiltonian (eq 1) is illustrated in Figure 1a. $\mathbf{S}_{i,b1}$ and $\mathbf{S}_{i,b2}$ are coupled by the intramolecular ferromagnetic exchange interaction, $J_1 > 0$, to give a molecular site of biradical or the two-spin site. The biradical spins are coupled with a neighboring monoradical spin of $S_{i,m} = {}^1/_2$ by the antiferromagnetic exchange interactions, J_2, J'_2, J_3, and J'_3. This is the simplest model Hamiltonian for molecular ferrimagnets possessing the above features, a biradical molecule with $\mathbf{S}_{i,b1} + \mathbf{S}_{i,b2}$ retaining the intramolecular magnetic degree of freedom, $J_1 \neq \infty$, and the 2-fold intermolecular interactions with the definable symmetry. The last term in eq 1 represents the Zeeman energy of the spins with the common g-factors, g.

Another type of a ferrimagnetic chain is compared with the molecule-based ferrimagnetic chain (eq 1). In transition metal compounds such as heterobimetallic chains of Ni^{2+} ($S = 1$) and Cu^{2+} ($S = {}^1/_2$),[4] any additional magnetic degrees of freedom within the $S > {}^1/_2$ ions are not considered except for the $2S + 1$ degeneracy. The spin Hamiltonian of the transition metal-based ferrimagnetic chain in the presence of applied static magnetic field, B, is given by

$$H_{atom} = \sum_{i=1}^{N}[-2J\mathbf{S}_{i,1}\cdot\mathbf{S}_{i,2} - 2J'\mathbf{S}_{i,2}\cdot\mathbf{S}_{i+1,1} + g\mu_B B(S^z_{i,1} + S^z_{i,2})] \quad (2)$$

where $\mathbf{S}_{i,1}$ and $\mathbf{S}_{i,2}$ denote the spin-1 and spin-${}^1/_2$ operators in the ith cell and N is the number of unit cells. The $S_{i,1} = 1$ and $S_{i,2} = {}^1/_2$ spins are coupled by the interatomic antiferromagnetic exchange interactions J and J'. The alternation or dimerization of the magnetic couplings along the chain is signified by the ratio J'/J. The third term in the Hamiltonian denotes the Zeeman interaction. The two kinds of spins, $S_{i,1} = 1$ and $S_{i,2} = {}^1/_2$, are assumed to have the same g-factors, g, for simplicity.

In our previous papers,[6-10] we discussed the possibility of ferrimagnetic order occurring in organic molecular assemblages both from numerical calculations of the spin Hamiltonian (eq 1)[6,8-10] and from crucial experiments[7] on the molecular complex mentioned above,[5] which is the only model compound reported so far. From a quantum Monte Carlo simulation of temperature dependence of the magnetic susceptibility, χ, the ground state of the Hamiltonian (eq 1) has been found to have the spin quantum number of $S = {}^N/_2$,[8] which is consistent with the theorem of Lieb and Mattis[11] for the collinear ferrimagnetic spin alignment in the Heisenberg system. An intuitive picture of the ferrimagnetic spin alignment in organic molecule-based or transition metal-based ferrimagnetic chains is a parallel alignment of resultant $S = {}^1/_2$ spins, which result from the antiparallel coupling of adjacent $S = 1$ and $S = {}^1/_2$ spins. The intuitive picture is given a rationale by the calculations of specific heat and entropy in the present study.

To our knowledge, theoretical physicists have proposed that the ferrimagnetic chains of $S = 1$ and $S = {}^1/_2$ (eq 2) have both ferromagnetic and antiferromagnetic natures in their thermodynamic behaviors.[12-20] Both ferromagnetic and antiferromagnetic branches of excitations have been found in the framework of a spin-wave theory.[13-20] In low-temperature regions, $k_BT \ll |J|$, the ferrimagnetic chain of $S = 1$ and $S = {}^1/_2$ (eq 2) behaves as an $S = {}^1/_2$ ferromagnetic chain, reflecting the structure of the dispersion relation of magnetic excitation. Effects of additional magnetic degrees of freedom have been overlooked in their studies. The present study shows a clear-cut molecule-based description of the ferrimagnetic spin alignment in terms of the effective $S = {}^1/_2$ spins composed of $S = 1$ and $S = {}^1/_2$ assemblages on the basis of the calculations of thermodynamic quantities and spin polarization effects inherent in molecular assemblages.

Methods of Computation

The magnetic specific heat of the multicentered ferrimagnetic chain was calculated by the exact numerical diagonalization of the Hamiltonian (eq 1) with the Householder method. The largest system examined in this study consists of four repeating units of a biradical and a monoradical (twelve $S = {}^1/_2$ spins) with the matrix dimension of $2^{12} \times 2^{12} = 4096 \times 4096$. The matrix was block-diagonalized according to the conservation of the z-component of the total spin. The periodic boundary condition $\mathbf{S}_{N+1,I} = \mathbf{S}_{1,I}$ (I = b1, b2, m) was imposed with $N = 4$ of repeating units in the Hamiltonian (eq 1).

The temperature dependence of the magnetic susceptibility χ was calculated by the quantum Monte Carlo simulation method of the loop algorithm, which is originally coded by M. Troyer at ETH Zurich.[21] In the calculations, a parallelization procedure was used on an NEC supercomputer SX-5 at the Research Center for Computational Science, Okazaki National Research Institute, and on a HITACHI supercomputer SR8000 at the Information Technology Center of the University of Tokyo. The minimum value of the product of susceptibility and temperature, χT_{min}, was calculated for $3N = 30$ of $S = {}^1/_2$ spins. The χT_{min} value for $3N = 30$ has been found to be identical to that for the longer chain of $3N = 60$[8] within a numerical accuracy. All of the calculations were made with $3N = 30$ to save CPU time.

The magnetic specific heat of the $S = 1$ and $S = {}^1/_2$ alternating chain was also calculated from the exact diagonalization of the Hamiltonian (eq 2). The first step of canonical orthogonalization[22] gave the eigenvectors of the square of the total spin, $[\sum(\mathbf{S}_{i,1} + \mathbf{S}_{i,2})]^2$, for the spin states of $S = 0$ to $S = 6$. Using the eigenvectors thus obtained, the Hamiltonian was diagonalized by the Householder method.

Results and Discussion

1. Transition Metal-Based Ferrimagnetic Spin Chains. The magnetic specific heat, C, of the $S = 1$ and $S = {}^1/_2$ ferrimagnetic chain was calculated from the thermodynamic average, $\langle E \rangle$, of the energy eigenvalues, E_i, of the spin Hamiltonian (eq 2)

$$\frac{C}{Nk_B} = \frac{1}{N(k_BT)^2}[\langle E^2\rangle - \langle E\rangle^2] \quad (3)$$

$$\langle E^2\rangle = \sum_i E_i^2 \exp(-E_i/(k_BT))/Z \quad (4)$$

$$\langle E\rangle = \sum_i E_i \exp(-E_i/(k_BT))/Z \quad (5)$$

where Z denotes the partition function:

$$Z = \sum_i \exp(-E_i/(k_BT)) \quad (6)$$

The summation i ran over $2^N \times 3^N$ states. The magnetic entropy, S_{mag}, was obtained by integrating numerically the specific heat:

$$S_{mag} = \int C/T \, dT \quad (7)$$

The high-temperature limit of the integral was normalized to ln 2 + ln 3

$$S_{mag}(T\rightarrow\infty)/(Nk_B) = \ln 2 + \ln 3 \quad (8)$$

which corresponds to the magnetic degree of freedom of $S = {}^1/_2$ and $S = 1$ in the unit cell. The number of the unit cells in the Hamiltonian was set to $N = 4$ in the calculations. This seems too small to deduce a quantitative conclusion. The temperature and field dependences of the specific heat for the $N = 4$ chain, however, reproduce those of longer chains obtained from a quantum Monte Carlo simulation[14] or those of a transfer matrix renormalization group theory.[15] We can discuss basic features of C *vs* T and S_{mag} *vs* T curves for the short ferrimagnetic chain. This is guaranteed by the extremely short spin−spin correlation length $\xi \approx 1/\ln 2$[23] of the ground-state correlation function $\langle S_i^z S_j^z\rangle$ for the chain.

The temperature dependence of the specific heat, C, and the entropy, S_{mag}, is drawn in Figure 2 as a function of the reduced temperature, $k_BT/(2|J|)$, and the reduced magnetic field defined as

$$h \equiv g\mu_B B/(2|J|) \quad (9)$$

For the uniform chain with a single interaction, J, a Schottky-like peak in C appears around $k_BT/(2|J|) \approx 0.6$ in the absence of the field $h = 0$ as shown in Figure 2a, which is designated "peak A". Around this temperature, the entropy, $S_{mag}/(Nk_B)$, is reduced from ln 2 + ln 3 to (ln 5)/4, which corresponds to the total spin of $S_T = 2$ for the whole chain with $N = 4$ in the ground state. The finite, nonzero entropy in the limit of zero temperature is due to the finite size of the system. The ferrimagnetic chain with N unit cells is expected to have a total spin of $S_T = N/2$,[8] and its entropy should be vanishing

$$S_{mag}(T\rightarrow 0)/N = \frac{\ln(2S_T+1)}{N} = \frac{\ln(N+1)}{N} \rightarrow 0 \quad (10)$$

in the thermodynamic limit of $N \rightarrow \infty$. The overall change in entropy is ln 2 + ln 3 for the ferrimagnetic chain of $S = 1$ and $S = {}^1/_2$ spin assemblages in the framework of the finite-size systems. This finding seems a matter of course. We find, however, the thermodynamic characteristics of the $S = 1$ and $S = {}^1/_2$ ferrimagnetic chain, when the alternation or dimerization is introduced to the magnetic couplings, J, along the chain. As depicted in Figure 3a, the alternating chain with the interaction parameters J and $J' = 0.1J$ exhibits a peak in C around $k_BT/(2|J|) \approx 0.6$, which is almost the same as peak A for the uniform chain. It should be noted that an additional peak in C appears around $k_BT/(2|J|) \approx 0.02$, which is called "peak B". The second peak at the lower temperature corresponds to a second drop in entropy, S_{mag}, as given in Figure 3b. The temperature dependence of entropy has a stationary behavior around $S_{mag}/(Nk_B) = \ln 2$. This indicates that an effective spin of $S = {}^1/_2$ appears in the unit cell of the chain in the stationary temperature region. An intuitive picture of the spin alignment in the ferrimagnetic chain is a parallel alignment of the resultant $S = {}^1/_2$ spins, which result from the antiparallel coupling of adjacent $S = 1$ and $S = {}^1/_2$ spins. The intuitive picture is rationalized by the stationary value of $S_{mag}/(Nk_B) = \ln 2$ in the unit cell.

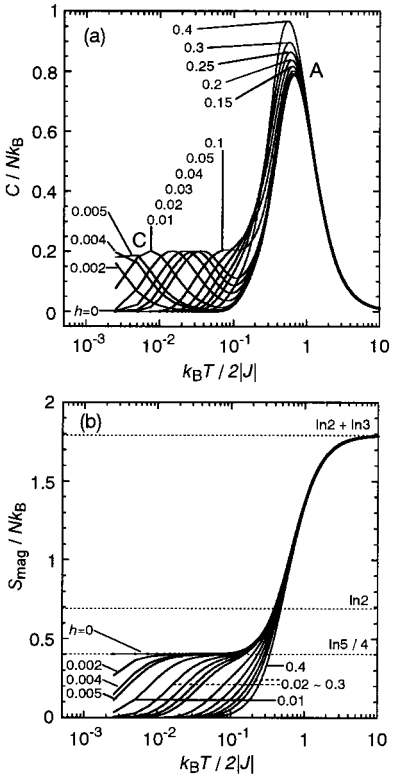

Figure 2. Magnetic specific heat, C (a), and entropy, S_{mag} (b), as functions of temperature, T, for the $S = 1$ and $S = {}^1/_2$ ferrimagnetic chain (Figure 1b; eq 2) with the number of unit cells $N = 4$. The antiferromagnetic interactions between the nearest-neighbor $S = 1$ and $S = {}^1/_2$ spins are uniform along the chain, $J'/J = 1$. The magnetic field, $h = g\mu_B B/(2|J|)$, ranges from zero up to 0.4. The horizontal dotted lines in panel b represent the entropy, $S_{mag}/(Nk_B)$, for free $S = {}^1/_2$ and $S = 1$ spins (ln 2 + ln 3), a free $S = {}^1/_2$ spin (ln 2) in the unit cell, and $S = 2$ in the whole chain ((ln 5)/4).

In an external magnetic field, an additional peak, "peak C", of specific heat appears as shown in Figures 2a and 3a. The peak shifts to higher temperatures as the magnetic field $h = g\mu_B B/(2|J|)$ is higher. The shift is indicative of the ferromagnetic nature of peak C; the Zeeman splittings of the low-lying spin states with nonzero S give the peaks. In the alternating chain with $|J'/J| = 0.1$, peak C merges with peak B and shifts to higher temperatures as the magnetic field is higher. On the other hand, peak A shifts to lower temperatures for the higher magnetic field, indicating the antiferromagnetic nature of the peak.

For ferrimagnetic spin chains of $S = {}^1/_2$ and $S = 1$ with uniform interatomic exchange interactions along the chain, a generic feature of two peaks in the temperature dependence of specific heat has been found from the transfer matrix renormalization group theory:[15] One peak with an antiferromagnetic nature appears at a higher temperature and shifts to lower

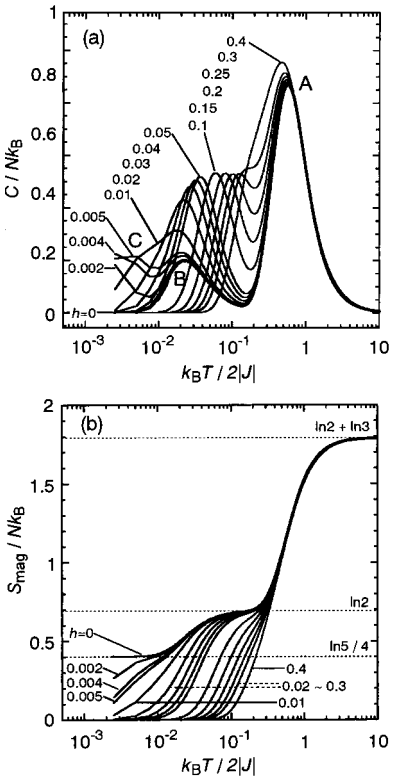

Figure 3. Magnetic specific heat, C (a), and entropy, S_{mag} (b), as functions of temperature, T, for the alternating or dimerized ferrimagnetic chain of $S = 1$ and $S = {}^1/_2$ (Figure 1b; eq 2). The degree of dimerization is $J'/J = 0.1$. The notations are the same as those in Figure 2.

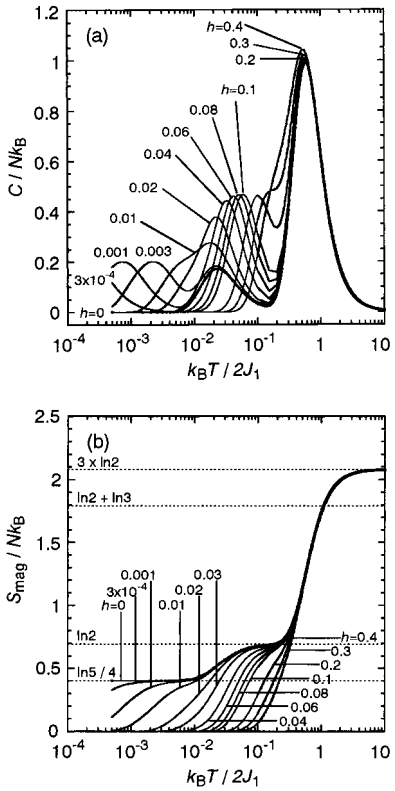

Figure 4. Magnetic specific heat, C (a), and entropy, S_{mag} (b), as functions of temperature, T, for the multicentered alternating ferrimagnetic chain (Figure 1a; eq 1). The intramolecular ferromagnetic interaction, J_1, is equal to the intermolecular antiferromagnetic interactions; $J_1 = |J_2| = |J_2'|$. The degree of dimerization of magnetic couplings along the chain is 1:${}^1/_{10}$; $J_3 = J_3' = J_2/10$. The horizontal dotted lines in panel b represent the entropy, $S_{mag}/(Nk_B)$, for three $S = {}^1/_2$ spins (3 ln 2), an $S = {}^1/_2$ and an $S = 1$ spin (ln 2 + ln 3), an $S = {}^1/_2$ spin (ln 2) in the unit cell, and $S = 2$ in the whole chain ((ln 5)/4). The magnetic field, $h = g\mu_B B/(2J_1)$, ranges from zero up to 0.1.

temperatures with applied static magnetic field.[15] The other appears at a lower temperature and exhibits a field-driven shift, indicating a ferromagnetic nature.[15] Both the peak height and the magnetic-field dependence of C in the present calculations for the small chain are almost the same as the above theories,[14,15] ruling out artifactual interpretation due to the insufficient system size. It is worth noting that the present calculations give the stationary behavior of the magnetic entropy at $S_{mag}/(Nk_B) = \ln 2$, which corresponds to the effective $S = {}^1/_2$ spin in the unit cells. The effective spins are coupled with each other by apparently ferromagnetic interactions, as indicated in the field dependence of the positions of peaks B and C.

2. Organic Molecule-Based Ferrimagnetic Spin Chains. *(a) Magnetic Specific Heat and Entropy.* The specific heat and the entropy of the molecule-based ferrimagnetic chain with three $S = {}^1/_2$ spins in the unit cell (eq 1) were calculated in the same way as those of the atom-based chain (eqs 2−8). Only the normalization condition, eq 8, was replaced by

$$S_{mag}(T\rightarrow\infty)/(Nk_B) = 3 \ln 2 \qquad (11)$$

for the high-temperature limit of the entropy, S_{mag}, as obtained from the integration of the specific heat, C, in accordance with the magnetic degree of freedom for the three $S = {}^1/_2$ spins in the unit cell. The magnetic field, B, is, as in eq 9 for the atom-based chains, normalized by J_1 and is expressed in a dimensionless form

$$h \equiv g\mu_B B/(2J_1) \qquad (12)$$

in the following calculations. In Figure 4a,b is depicted the temperature dependence of the specific heat and entropy for the multicentered alternating chain (eq 1) with the number of the unit cells $N = 4$. Here, the intramolecular ferromagnetic interaction J_1 is equal to the intermolecular antiferromagnetic interactions; $J_1 = |J_2| = |J_2'|$. The degree of dimerization of magnetic couplings along the chain is 1:0.1; $J_3 = J_3' = J_2/10$.[24] In these conditions, the specific heat, C, exhibits a couple of peaks at $k_BT/(2J_1) \approx 0.6$ and $k_BT/(2J_1) \approx 0.02$ in the absence of the magnetic field, $h = 0$. At these temperatures, the entropy, $S_{mag}/(Nk_B)$, drops from 3 ln 2 to ln 2 and ln 2 to (ln 5)/4 as illustrated in Figure 4b. The temperature dependence of the specific heat and the entropy is quite similar to that of the metal-based alternating chain, as shown in Figure 3. An effective $S = {}^1/_2$ spin with the entropy of $S_{mag}/(Nk_B) = \ln 2$ appears in the intermediate regions of temperature. The response to the magnetic field is also similar to that of the metal-based chain: A third peak appears in response to a weak field, $h = 3 \times 10^{-4}$. As the field is increased, the peak shifts to higher temperatures and merges into the second peak at $h = 0.02$.

Interestingly, the thermodynamic properties of the multicentered ferrimagnetic chain are quite different from the cases discussed above, when the intramolecular ferromagnetic interaction J_1 is much larger than the intermolecular antiferromagnetic interactions. One finds three distinguishable peaks in the C vs T curve as shown in Figure 5a. The peak in C at the highest temperature ($k_BT/(2J_1) \approx 0.5$) is associated with a decrease in $S_{mag}/(Nk_B)$ down to ln 2 + ln 3 (Figure 5b). This entropy corresponds to the generation of an $S = {}^1/_2$ spin and an $S = 1$ spin in the unit cell. Thus, the peak at $k_BT/(2J_1) \approx 0.5$ is a Schottky-type originating from the intramolecular singlet−triplet

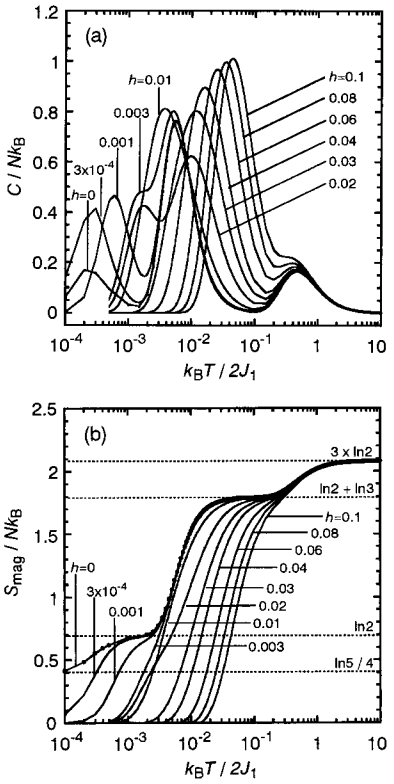

Figure 5. Magnetic specific heat, C (a), and entropy, S_{mag} (b), as functions of temperature, T, for the multicentered alternating ferrimagnetic chain (Figure 1a; eq 1). The intramolecular ferromagnetic interaction, J_1, is much larger than the intermolecular antiferromagnetic interactions; $J_1 = 100|J_2| = 100|J_2'|$. The degree of dimerization of magnetic couplings along the chain is $1:^1/_{10}$; $J_3 = J_3' = J_2/10$. The other notations are the same as those in Figure 4.

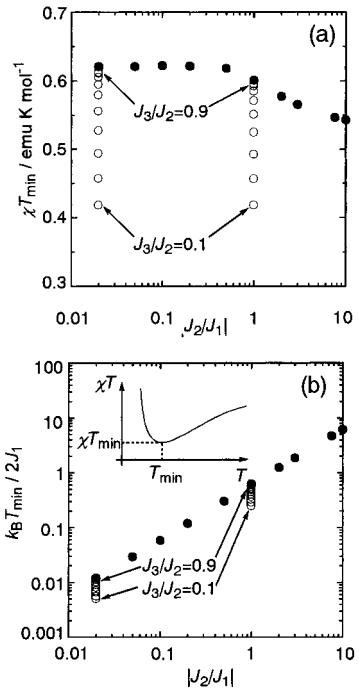

Figure 6. Magnetic susceptibility, χ, of the molecule-based ferrimagnetic chain in Figure 1a simulated by the quantum Monte Carlo method: (a) χT_{min}; (b) T_{min}. The definition of χT_{min} and T_{min} is indicated in the inset. The solid symbols denote the uniform chain ($J_3/J_2 = J_3'/J_2' = 1$), while the open ones represent the dimerized chains with the alternation of $J_3/J_2 = J_3'/J_2' = 0.1-0.9$.

energy gap $2J_1$ in the biradical. Little temperature shift with the magnetic field is found for the intramolecular Schottky peak, which is consistent with the low magnetic field, $g\mu_B B \ll 2J_1$, examined. The other two peaks at the lower temperature have the same physical origin as peaks A and B for the metal-based chain with the dimerization of magnetic couplings along the chain, as given in Figure 3a,b. An effective $S = {}^1/_2$ spin with the entropy of $S_{mag}/(Nk_B) = \ln 2$ in the unit cell is found as well in the intermediate temperature region $k_BT/(2J_1) \approx 0.01$. Similar shifts of the peaks are also found in response to the magnetic field: According to the energy scales of intermolecular or interatomic interactions along the chain, the ranges of temperature and magnetic field giving the shifts for peak A, $k_BT/(2|J|) \approx 0.6$ at $h = 0.1-0.4$ for the atom-based chain, correspond to those of the second peak for the multicentered chain, $k_BT/(2|J_1|) \approx 0.006$ at $h = 0.003-0.01$.

(b) Magnetic Susceptibility. Low-dimensional ferrimagnetic spin systems have been known to exhibit a minimum and a divergence in χT as the temperature approaches zero.[4,8,14,17] It is crucially important how the divergent behavior of χT is affected by the ratio of multicentered or multicontact exchange interactions in the organic molecule-based ferrimagnetic chains. For low-dimensional antiferromagnetic spin systems, a minimum in χ or χT usually has a simple linear dependence on the relevant exchange interaction constants.[25] From simulations of the minimum value of χT_{min} and the temperature, T_{min}, effects of the exchange interactions on the divergent behavior of χT are examined in this section.

The temperature dependence of χT is calculated in terms of a quantum Monte Carlo simulation[8,21] of the Hamiltonian (eq 1). In Figure 6 are plotted the χT_{min} (a) and T_{min} values (b) as functions of the interaction ratio $|J_2/J_1|$. Simulations for very weak intermolecular interactions, $|J_2/J_1| < 0.01$, were difficult to obtain, because the resultant low T_{min} values prevented numerical convergence in χ with a satisfactory accuracy. The solid symbols in Figure 6a denote the χT_{min} values calculated for the uniform chain ($J_3/J_2 = J_3'/J_2' = 1$). When the intermolecular interactions are weak ($|J_2/J_1| < 0.5$), the χT_{min} value is independent of $|J_2/J_1|$. As the intermolecular interactions become larger ($|J_2/J_1| > 0.5$), the χT_{min} value decreases. The dimerization, or the alternation, of the intermolecular interactions along the chain results in a drop in χT_{min}, as shown by the open symbols in Figure 6a for $0.1 \le J_3/J_2 \le 0.9$ in the regions of both $|J_2/J_1| < 0.5$ and $|J_2/J_1| > 0.5$. The temperature giving the χT minimum, $k_BT_{min}/(2J_1)$, is approximately linear with respect to the intermolecular interaction $|J_2/J_1|$, as depicted by the solid symbols in Figure 6b. For the chain with $|J_2/J_1| = 1$ and the alternation of 1:0.1, χT takes a minimum at $k_BT_{min}/(2J_1) \approx 0.25$, where the entropy, $S_{mag}/(Nk_B)$, reaches ln 2. The minimum and upturn in χT on lowering the temperature originate in the generation of the effective $S = {}^1/_2$ spin with effective ferromagnetic interactions.

As the interaction ratio, J_3/J_2 ($= J_3'/J_2'$), deviates from unity and approaches zero, the alternating molecular chain of the biradicals and the monoradicals should be regarded as an assemblage of biradical−monoradical pairs, in which the interactions between the pairs, J_3 or J_3', are negligible. In the pair, the biradical and the monoradical are coupled by the antiferromagnetic interaction, J_2 or J_2', to give a supramolecule in the doublet ($S = {}^1/_2$) state; there appears an effective $S = {}^1/_2$ spin in the unit cell of the chain. The assemblage of the $S = {}^1/_2$ spins is consistent with the limiting value of $\chi T_{min} \rightarrow 0.38$ emu K mol^{-1} for $J_3/J_2 (= J_3'/J_2') \rightarrow 0$, as shown in Figure 6a. This behavior corresponds to the Curie law of $S = {}^1/_2$ with $g = 2.0$.

(c) Spin Polarization in the Pair of a Spin-1 Biradical and a Spin-$^1/_2$ Monoradical. Intermolecular ferromagnetic interactions

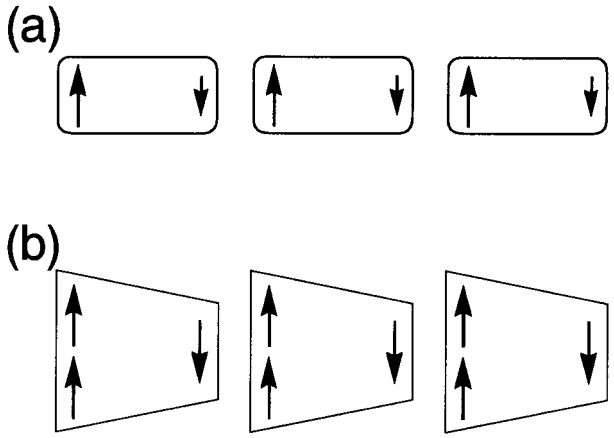

Figure 7. Schematic diagrams for the spin polarization in the $S = {}^1/_2$ ferromagnetic chain (a) and the dimerized chain of biradicals and monoradicals (b). The arrows indicate the positive or negative spin polarization.

between $S = {}^1/_2$ organic radicals have been understood in terms of the spin polarization effect within the $S = {}^1/_2$ molecules.[26,27] The spin polarization provides the spin density distribution with positive and negative signs in the molecule. Intermolecular orbital overlaps between neighboring molecules at the atomic sites of opposite signs of spin densities give rise to a ferromagnetic interaction between the molecules, which is schematically shown in Figure 7a.

The spin state of a supramolecule composed of a ground-state triplet ($S = 1$) biradical and an $S = {}^1/_2$ monoradical is doublet ($S = {}^1/_2$) or quartet ($S = {}^3/_2$). Intermolecular antiferromagnetic interactions within the pair give the doublet ($S = {}^1/_2$) ground state of the supramolecule. The supramolecule in the $S = {}^1/_2$ ground state should have the resultant positive spin density in the biradical moiety, while the resultant negative spin density should appear preferentially in the monoradical moiety. The spin density distribution or the spin polarization in the supramolecule is deduced from the Heisenberg model:

$$H_{\text{pair}} = -2j_1\mathbf{S}_{\text{b1}}\cdot\mathbf{S}_{\text{b2}} - 2j_2\mathbf{S}_{\text{b2}}\cdot\mathbf{S}_{\text{m}} - 2j_2'\mathbf{S}_{\text{b1}}\cdot\mathbf{S}_{\text{m}} \quad (13)$$

which corresponds to the Heitler−London model applied to the supramolecule and is equivalent to the unit cell of the chain Hamiltonian (eq 1). The ferromagnetic interaction j_1 and the antiferromagnetic interactions j_2 and j_2' give the doublet ($S = {}^1/_2$) ground state. When j_2 is equal to j_2', the spin operator of the biradical $(\mathbf{S}_{\text{b1}} + \mathbf{S}_{\text{b2}})^2$ commutes with the Hamiltonian (eq 13)[8,9] and then the spin function Ψ of the $M_S = {}^1/_2$ component for the doublet ground state is given from the Clebsh−Gordon coefficients for the coupling of an $S = 1$ and an $S = {}^1/_2$ spin angular momentum:

$$\Psi = \sqrt{\frac{1}{6}}(\alpha_{\text{b1}}\beta_{\text{b2}}\alpha_{\text{m}} + \beta_{\text{b1}}\alpha_{\text{b2}}\alpha_{\text{m}}) - \sqrt{\frac{2}{3}}\alpha_{\text{b1}}\alpha_{\text{b2}}\beta_{\text{m}} \quad (14)$$

where α and β are the up- and down-spin functions of $S = {}^1/_2$, respectively. The spin densities of the three molecular sites, b1, b2, and m, are deduced from eq 14 as

$$\langle S_{\text{b1}}^z\rangle = \langle S_{\text{b2}}^z\rangle = {}^1/_3, \quad \langle S_{\text{m}}^z\rangle = -{}^1/_6 \quad (15)$$

The monoradical moiety in the supramolecule has the resultant negative spin density, $-{}^1/_6$. This is the same as that of the central carbon atom of allyl radical in the simple valence-bond picture or the Heisenberg model.[28] For arbitrary values of $j_2 \neq j_2'$, the biradical spin, $(\mathbf{S}_{\text{b1}} + \mathbf{S}_{\text{b2}})^2$, does not commute with the Hamiltonian (eq 13).[8,9] Then, the spin function was calculated by diagonalizing the Hamiltonian, which gave the spin densities of the three molecular sites:

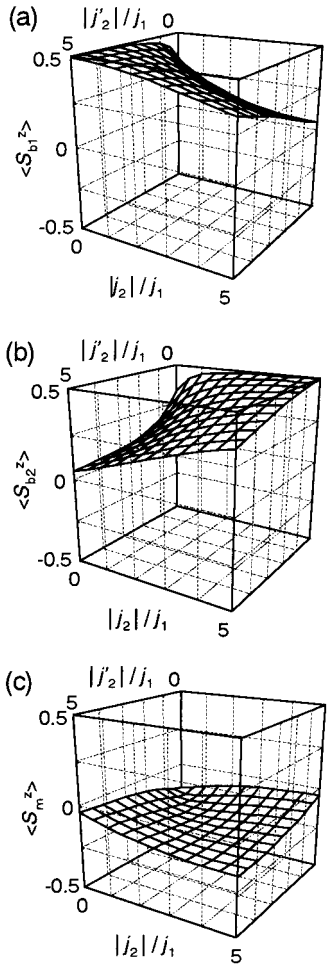

Figure 8. The spin polarization, $\langle S_{\text{b1}}^z\rangle$, $\langle S_{\text{b2}}^z\rangle$, and $\langle S_{\text{m}}^z\rangle$, in the doublet ground state of the pair of a biradical and a monoradical (H_{pair}, eq 13).

$$\langle S_{\text{b1}}^z\rangle = {}^1/_6\{1 + (j_1 - 2j_2 + j_2')/A\} \quad (16a)$$

$$\langle S_{\text{b2}}^z\rangle = {}^1/_6\{1 + (j_1 + j_2 - 2j_2')/A\} \quad (16b)$$

$$\langle S_{\text{m}}^z\rangle = {}^1/_6\{1 + (-j_1 + j_2 + j_2')/A\} \quad (16c)$$

$$A = \sqrt{j_1^2 + j_2^2 + j_2'^2 - j_1j_2 - j_1j_2' - j_2j_2'} \quad (16d)$$

As shown in Figure 8, for arbitrary values of $j_1 > 0$, $j_2 < 0$, and $j_2' < 0$, we find positive spin densities, $\langle S_{\text{b1}}^z\rangle > 0$ and $\langle S_{\text{b2}}^z\rangle > 0$, at the biradical sites and a negative spin density, $\langle S_{\text{m}}^z\rangle < 0$, at the monoradical site. The largest negative spin polarization is found along the diagonals of the $\{|j_2|/j_1, |j_2'|/j_1\}$ plane; $\langle S_{\text{m}}^z\rangle = -{}^1/_6$. Although we notice that the Heitler−London approach overestimates the amplitude of spin polarization, the polarization in the three-spin system gives ferromagnetic interactions between the supramolecules in the alternating chain, as shown in Figure 7b. Thus, the ferrimagnetic spin state in the alternating chain of the biradicals and monoradicals is equivalent to the ferromagnetic alignment of $S = {}^1/_2$ spins on the spin-polarized supramolecules for highly dimerized intermolecular interactions along the chain. The effective $S = {}^1/_2$ spin with the entropy of k_{B} ln 2 has been found in the calculations of C vs T and S_{mag} vs

T curves, which have exhibited the magnetic field dependence of the ferromagnetic nature. The effective $S = {}^1/_2$ spin is attributable to the spin-polarized supramolecule.

It should be noted that the signs of the spin densities at the three molecular sites (eq 16) are invariable in the limit of $j_1 \rightarrow 0$: The spin polarization in the pair, $\langle S^z_{b1} \rangle > 0$, $\langle S^z_{b2} \rangle > 0$, and $\langle S^z_m \rangle < 0$, is retained as long as the antiferromagnetic interactions j_2 and j_2' are operative. Therefore, an extended chain with vanishing J_1, which is regarded as an array of vertex-sharing diamonds of exchange-coupled spins ($J_1 = 0$ in Figure 1a), can give the ferrimagnetic ground state as well. In this context, an inorganic complex[29] of Cu(II) with $S = {}^1/_2$ is interesting, which possesses the vertex-sharing diamond structure of $S = {}^1/_2$ spins. The complex has exhibited a divergence in χT at low temperatures, indicating the occurrence of a ferrimagnetic ground state of the chain.[29,30] Only the topology[31] of the antiferromagnetic interactions between the $S = {}^1/_2$ spins is responsible for the ferrimagnetic spin alignment. Two extreme cases of $J_1 \approx |J_2|, |J_3|$ (the biradical−monoradical molecular chain) and $J_1 = 0$ (the three-centered $S = {}^1/_2$ spin system of the Cu complex or the allyl radical) are understood on the single basis of the exchange coupling model (eqs 1 and 13): the former includes the latter. The general molecule-based description of the ferrimagnetic spin alignment, as proposed from calculations of thermodynamic properties and the spin polarization, uncovers new quantum aspects of magnetism, contributing to new molecular designing of molecular magnetic materials.

Conclusion

The ferrimagnetic spin alignment in the organic molecule-based quantum spin chains has theoretically been studied and compared with that in the atom-based chains in terms of thermodynamic properties. The intermolecular or interatomic antiferromagnetic interactions along the chains give the Schottky-like peak of specific heat, *C*, in both atom-based and molecule-based multicentered ferrimagnetic chains. The introduction of dimerization or alternation of magnetic interactions along the chain gives rise to the second peak in the *C* vs *T* curves at a lower temperature. This is attributed to the generation of an effective $S = {}^1/_2$ spin in the unit cell. The change in entropy, S_{mag}, associated with the effective $S = {}^1/_2$ spin is distinguishable from the overall change by the introduction of the dimerization. When the intramolecular ferromagnetic interaction in the biradical is much larger than the intermolecular interactions, further distinction of entropy change is found in the molecular ferrimagnetic chain. The molecule-based multicentered ferrimagnetic spin system is characterized by the three peaks in specific heat and the associated 3-fold drops in entropy. This reflects the internal magnetic degree of freedom in the ground-state triplet ($S = 1$) molecules. Although the three peaks in the specific heat are difficult to observe in experiments owing to the lattice contribution of specific heat at high temperatures, the spin alignment in the multicentered, multispin systems is made readily understandable in terms of magnetic entropy.

The description of the effective $S = {}^1/_2$ spins on the supramolecules is valid only for highly dimerized intermolecular interactions along the chain, $J_3/J_2 = J_3'/J_2' \ll 1$, where the effective $S = {}^1/_2$ spin is a good quantum number for describing the magnetic properties of the unit cell in the molecular chain. The intermolecular interactions for the supramolecules with the effective $S = {}^1/_2$ spins govern the temperature at which the ferrimagnetic spin−spin correlation develops in the assemblage of the supramolecules. In higher dimensional lattices, the transition temperature to a possible ferrimagnetic ordered state should be governed by the interactions between the supramolecules. Therefore, elaborate control or tuning of the intra- and intermolecular interactions is necessary to accomplish the ferrimagnetic spin alignment at high temperatures, which is based on the spin polarization within the organic open-shell molecules and molecular packings governing the intermolecular interactions. The thermodynamic properties acquired in the present study will be useful for analyzing experimental results on real organic molecular ferrimagnets appearing in the future and, in turn, the theoretical model will be improved from the simplest form (eq 1) to a more sophisticated one on the basis of the experimental results, serving for a breakthrough of organic molecule-based ferrimagnetics.

Acknowledgment. This work has been supported by Grants-in-Aid for Encouragement of Young Scientists (Grant Nos. 07740468, 07740553, 08740462, 09740528, 10740275, and 12740385) and Grants-in-Aid for Scientific Research from the Ministry of Education, Sports, Culture Science and Technology, Japan.

References and Notes

(1) For reviews of molecule-based magnetism, see: (a) Gatteschi, D., Kahn, O., Miller, J. S., Palacio, F., Eds. *Molecular Magnetic Materials*; Kluwer Academic: Dordrecht, Netherlands, 1991. (b) Iwamura, H.; Miller, J. S. *Mol. Cryst. Liq. Cryst. Sci. Technol. Sect. A* **1993**, *232*, *233*. (c) Miller, J. S.; Epstein, A. J. *Mol. Cryst. Liq. Cryst. Sci. Technol. Sect. A* **1995**, *271*−*274*. (d) Itoh, K.; Miller, J. S., Takui, T. *Mol. Cryst. Liq. Cryst. Sci. Technol. Sect. A* **1997**, *305*, *306*. (e) Kahn, O. *Mol. Cryst. Liq. Cryst. Sci. Technol. Sect. A* **1999**, *334*, *335*. (f) Lahti, P. M., Ed. *Magnetic Properties of Organic Materials*; Marcel Dekker: New York, 1999. (g) Itoh, K., Kinoshita, M., Eds. *Molecular Magnetism*; Gordon and Breach: Amsterdam (Kodansha: Tokyo), 2000.

(2) (a)Tamura, M.; Nakazawa, Y.; Shiomi, D.; Nozawa, K.; Hosokoshi, Y.; Ishikawa, M.; Takahashi, M.; Kinoshita, M. *Chem. Phys. Lett.* **1991**, *186*, 401. (b) Nakazawa, Y.; Tamura, M.; Shirakawa, N.; Shiomi, D.; Takahashi, M.; Kinoshita, M.; Ishikawa, M. *Phys. Rev. B* **1992**, *46*, 8906.

(3) Buchachenko, A. L. *Dokl. Phys. Chem. (Transl. of Dokl. Akad. Nauk.)* **1979**, *244*, 107.

(4) For example, see: (a) Kahn, O.; Pei, Y.; Verdaguer, M.; Renard, J. P.; Sletten, J. *J. Am. Chem. Soc.* **1988**, *110*, 782. (b) Caneschi, A.; Gatteschi, D.; Renard, J. P.; Rey, P.; Sessoli, R. *Inorg. Chem.* **1989**, *28*, 1976. (c) Stumpf, H. O.; Ouahab, L.; Pei Y.; Bergerat, P.; Kahn, O. *J. Am. Chem. Soc.* **1994**, *116*, 3866. (d) Hagiwara, M.; Minami, K.; Narumi, Y.; Tatani, K.; Kindo, K. *J. Phys. Soc. Jpn.* **1998**, *67*, 2209. (e) Hagiwara, M.; Narumi, Y.; Minami, K.; Tatani, K.; Kindo, K. *J. Phys. Soc. Jpn.* **1999**, *68*, 2214.

(5) Izuoka, A.; Fukada, M.; Kumai, R.; Itakura, M.; Hikami, S.; Sugawara, T. *J. Am. Chem. Soc.* **1994**, *116*, 2609.

(6) Shiomi, D.; Nishizawa, M.; Sato, K.; Takui, T.; Itoh, K.; Sakurai, H.; Izuoka, A.; Sugawara, T. *J. Phys. Chem. B* **1997**, *101*, 3342.

(7) Nishizawa, M.; Shiomi, D.; Sato, K.; Takui, T.; Itoh, K.; Sawa, H.; Kato, R.; Sakurai, H.; Izuoka, A.; Sugawara, T. *J. Phys. Chem. B* **2000**, *104*, 503.

(8) Shiomi, D.; Sato, K.; Takui, T. *J. Phys. Chem. B* **2000**, *104*, 1961.

(9) Shiomi, D.; Sato, K.; Takui, T. *J. Phys. Chem. B* **2001**, *105*, 2932.

(10) Shiomi, D.; Nishizawa, M.; Sato, K.; Mito, M.; Takeda, K.; Takui, T. *Mol. Cryst. Liq. Cryst. Sci. Technol. Sect. A*, in press.

(11) Lieb, E.; Mattis, D. *J. Math. Phys.* **1962**, *3*, 749.

(12) Kolezhuk, A. K.; Mikeska, H.-J.; Yamamoto, S. *Phys. Rev. B* **1997**, *55*, R3336.

(13) Yamamoto, S.; Brehmer, S.; Mikeska, H.-J. *Phys. Rev. B* **1998**, *57*, 13610.

(14) Yamamoto, S.; Fukui, T. *Phys. Rev. B* **1998**, *57*, R14008.

(15) Maisinger, K.; Schollwock, U.; Brehmer, S.; Mikeska, H.-J.; Yamamoto, S. *Phys. Rev. B* **1998**, *58*, R5908.

(16) Yamamoto, S.; Sakai, T. *J. Phys. Soc. Jpn.* **1998**, *67*, 3711.

(17) Yamamoto, S. *Phys. Rev. B* **1999**, *59*, 1024.

(18) Sakai, T.; Yamamoto, S. *Phys. Rev. B* **1999**, *60*, 4053.

(19) Yamamoto, S. *Phys. Rev. B* **2000**, *61*, R842.

(20) Yamamoto, S. *J. Phys. Soc. Jpn.* **2000**, *69*, 2324.

(21) Troyer, M.; Ammon, B.; Heeb, E. Caromel, D. *Lecture Notes in Computer Science*; Springer: Berlin, 1999; p 191.

(22) Szabo, A.; Ostlund, N. S. *Modern Quantum Chemistry: Introduction to Advanced Electronic Structure Theory*; Macmillan: Indianapolis, IN, 1982; Chapter 3.

(23) Pati, S. K.; Ramasesha, S.; Sen, D. *Phys. Rev. B* **1997**, *55*, 8894.

(24) The spatial symmetry of the 2-fold intermolecular interactions along the chain is neglected in the present study. The influence of the symmetry between the $\mathbf{S}_{i,b1}\cdot\mathbf{S}_{i,m}$ and $\mathbf{S}_{i,b2}\cdot\mathbf{S}_{i,m}$ pairs, or the ratio J_2'/J_2, and between the $\mathbf{S}_{i,m}\cdot\mathbf{S}_{i+1,b1}$ and $\mathbf{S}_{i,m}\cdot\mathbf{S}_{i+1,b2}$ pairs, or the ratio J_3'/J_3, in the Hamiltonian (eq 1) on the thermodynamic properties will be discussed in a separate paper.

(25) de Jongh, L. J.; Miedema, A. R. *Adv. Phys.* **1974**, *23*, 1.

(26) McConnell, H. M. *J. Chem. Phys.* **1963**, *39*, 1910.

(27) Awaga, K.; Sugano, T.; Kinoshita, M. *Chem. Phys. Lett.* **1987**, *141*, 540.

(28) For example, see: Kahn, O. *Molecular Magnetism*; VCH: New York, 1993; p 307.

(29) Drillon, M.; Belaiche, M.; Legoll, P.; Aride, J.; Boukhari, A.; Moqine, A. *J. Magn. Magn. Mater.* **1993**, *128*, 83.

(30) In ref 29, theoretical calculations of specific heat have been made for the vertex-sharing diamond structure using an Ising-type and a Heisenberg-type spin Hamiltonian. A couple of peaks in the *C* vs *T* curve have been found in the calculations. Nevertheless, the physical origin of the appearance of the two peaks has not been clarified in terms of magnetic entropy.

(31) The topology of the antiferromagnetic couplings discussed in ref 29 is not exactly the same as ours in Figure 1a. The alternation of magnetic couplings in the former undergoes criss-cross coupling topology and twists along the chain.